ANNUAL SPATIAL VARIABILITY OF THE HYDROGRAPHIC STRUCTURE ALONG THE SEWARD LINE: PRELIMINARY RESULTS

Isaac D. Schroeder • Chester E. Grosch • Thomas C. Royer

Center for Coastal Physical Oceanography, Department of Ocean, Earth and Atmospheric Sciences, Old Dominion University, Norfolk, VA 23529

INTRODUCTION

Normal Mode Analysis (NMA) of GLOBEC hydrographic data (temperature, salinity, and density) along the Seward Line has been used for the detection of dominant spatial modes. The GLOBEC data was collected over 20 cruises from October 1997 to April 2001.

Normal Mode Analysis (NMA)

To perform NMA, a grid is constructed that divides the domain into equally spaced horizontal and equally spaced vertical divisions. There are a total of 27 x_i grid points and 44 y_k grid points. The horizontal grid is 216 kilometers long and the vertical grid is 215 meters deep. The inner and outer boundaries are the stations at GAK 1 and GAK 13; the top boundary is at 5 m below the surface and the bottom boundary is at 220 m.

Spatial eigenfunctions on this grid are calculated by solving Helmholtz's equation with Dirichlet boundary conditions. It can be shown that the infinite set of eigenfunctions is complete for any smooth function which is zero on the boundaries. In addition, a boundary solution, $\Theta\ (x_j, y_k, t_i)$, must be calculated to account for the nonzero values of the temperature, salinity and density on the boundaries. This is done separately for each set of hydrographic data for a particular cruise time denoted by t_i. The boundary solution is calculated by solving Laplace's equation on the domain with the data on the boundary giving the boundary conditions. The theory of NMA for scalar fields, as here, is given by Eremeev et al., 1995, and the extension to vector fields by Lipphardt et al., 2000.

A set of 78 eigenfunctions, in addition to the boundary solution, were calculated at the discrete x_i and y_k values. These eigenfunctions are called **Dirichlet modes** and are denoted by $\Psi_n(x_j, y_k)$, where n is the mode number and ranges from 1 to 78.
The Dirichlet modes have a maximum of 13 horizontal divisions and 6 vertical divisions. The following name convention is used to distinguish between sets of 13 modes:

a) **Barotropic group:** Dirichlet modes 1 through 13
b) **1st Baroclinic group:** Dirichlet modes 14 through 26
c) **2nd Baroclinic group:** Dirichlet modes 27 through 39
d) **3rd Baroclinic group:** Dirichlet modes 40 through 52
e) **4th Baroclinic group:** Dirichlet modes 53 through 65
f) **5th Baroclinic group:** Dirichlet modes 66 through 78

For a set of hydrographic data at a particular cruise date, t_i, the boundary solution is calculated and subtracted from the data. Next, the **amplitude** of each of the 78 modes is calculated by doing a least squares projection of the data onto the set of modes yielding an amplitude array, A_n, 78 elements long. Repeating this for each of the 20 cruises yields a time series of the amplitudes of each mode denoted by $A_n\ (t_i)$.

The original scalar field for a particular time can be reconstructed by calculating a **nowcast**. A nowcast can be performed by summing all of the products of the Dirichlet mode with its corresponding mode amplitude and adding the boundary solution:

$$Nowcast\ (x_j, y_k, t_i) = \sum_{n=1}^{78} A_n\ (t_i)\ \Psi_n(x_j, y_k) + \Theta\ (x_j, y_k, t_i).$$

This, in effect, is a lowpass spatial filtering of the data.

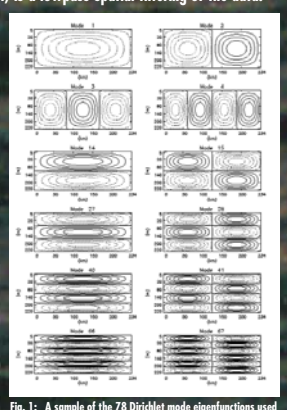

Fig. 1: A sample of the 78 Dirichlet mode eigenfunctions used for the NMA. The dashed lines are positive values and the solid lines are negative values.

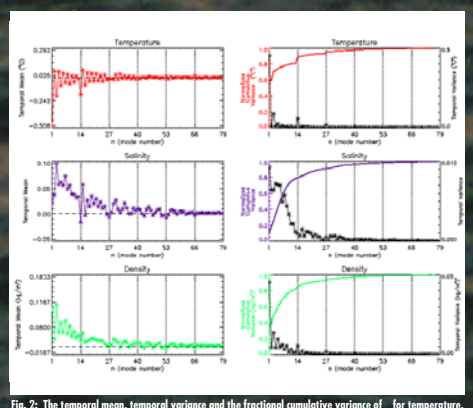

Fig. 2: The temporal mean, temporal variance and the fractional cumulative variance of for temperature, salinity and density.

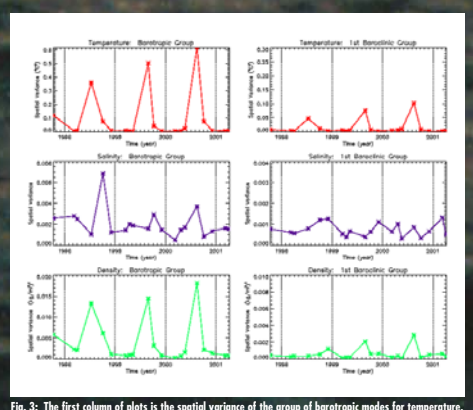

Fig. 3: The first column of plots is the spatial variance of the group of barotropic modes for temperature, salinity and density. The second column of is the spatial variance of the group of first baroclinic modes for temperature, salinity and density.

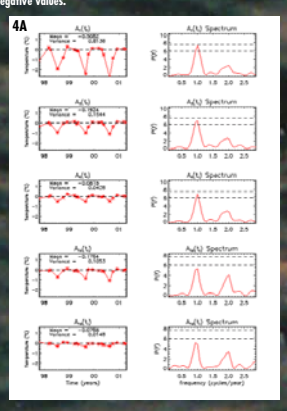

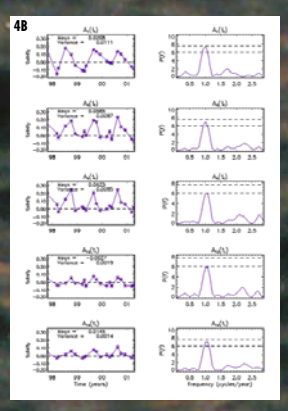

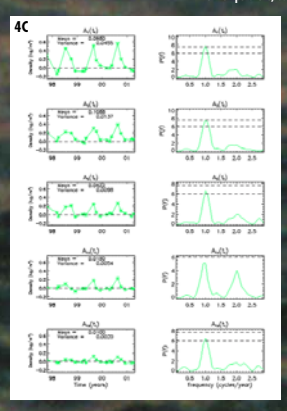

Fig. 4: The first column of plots is the time series of the amplitude for a particular mode, and the second column is the corresponding Lomb's spectrum. The first three modes displayed are the modes with the largest variance in the barotropic group and the last two are the modes with the largest variance in the first baroclinic group.
Fig 4a: Modes 1, 3, 5, 14 and 16 for temperature.
Fig 4b: Modes 1, 4, 5, 16 and 18 for salinity.
Fig 4c: Modes 1, 3, 5, 14 and 16 for density.

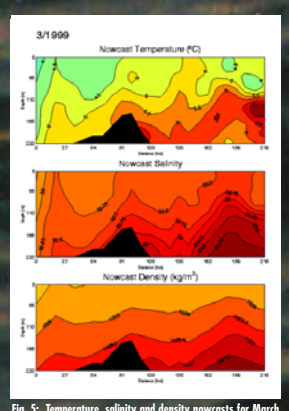

Fig. 5: Temperature, salinity and density nowcasts for March 1999.

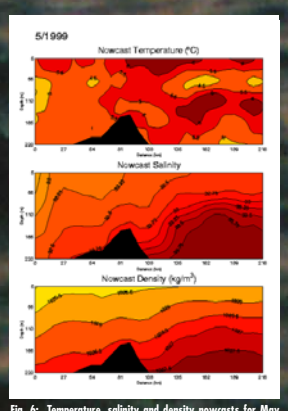

Fig. 6: Temperature, salinity and density nowcasts for May 1999.

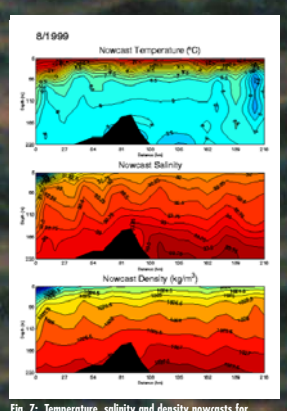

Fig. 7: Temperature, salinity and density nowcasts for August 1999.

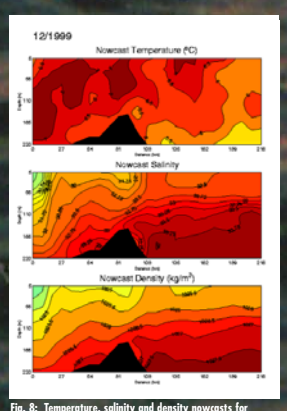

Fig. 8: Temperature, salinity and density nowcasts for December1999.

RESULTS

Figure 1 is a sub sample of the 78 entire Dirichlet modes. The first four plots show contours of the first four purely barotropic (vertically uniform) eigenfunctions. The remaining plots show contours of the first 2 eigenfunctions of the 1st through 4th baroclinic groups. Note that modes 14, 27, 40 and 66 are purely baroclinic (vertically structured) while the others have a mixed structure. The dashed lines are positive values and the solid lines are negative values.

Figure 2 shows the temporal mean, temporal variance and fractional cumulative variance of the time series of the amplitudes of the 78 modes for the temperature, salinity and density fields. The temperature and salinity modes have different amplitude variations. The barotropic temperature modes 1 and 3 and the first baroclinic mode, 14, have the largest means and modes 1 and 3 have the largest variance with about 75% of the variance being explained by these two modes. In contrast, the first 13 (barotropic) salinity modes all have relatively large means as do the baroclinic modes 15, 17-25, 29, 30 and 34. The variance of the salinity modes is more "broad band" than that of the temperature with modes 1 through 12 making significant contributions as shown by having the first 14 modes explain 80% of the variance. The density, of course, reflects a mixture of the temperature and salinity modes with the salinity having a greater effect as shown by the fact that the first 11 density modes are needed to account for 80% of the variance.

For the temperature and density, modes 1 and 3 contain most of the variance (Fig. 2, second column). Also the sign of the mean for modes 1 and 3 are both negative for temperature and positive for density (Fig. 2, first column). Looking at Dirichlet modes 1 and 3 (Fig. 1) shows that mode 1 has a positive peak in the center and mode 3 has a negative peak in the center flanked by positive peaks. Since the sign of the amplitude is the same for mode 1 and mode 3, when these two modes are summed together the resulting scalar field will be more horizontally uniform.

Figure 3 shows the time series of the spatial variance of the group of barotropic modes and the first group of baroclinic modes; the other groups of baroclinic modes do not contribute significantly to the total variance. For the temperature, these two groups both show a strong annual signal with the maximum amplitude increasing over the period from late 1998 to 2001. For salinity the time series of the variance of both the group of barotropic and first baroclinic modes are, in contrast to temperature, much more constant. There is only a single large peak in the barotropic salinity variance in late 1998. This peak might be explained by the relatively large negative discharge anomaly at the end of 1998. The time series of the density modes reflect the mixture of the temperature and salinity modes. The annual signal is seen in both groups of modes with a modest increase in the magnitudes of the annual signals.

Time series of some of the more significant modes amplitudes are shown in Figure 4 (Fig. 4a temperature, 4b salinity and 4c density). In addition, the mean and variance of each mode's time series is given. Alongside each time series plot is the power spectrum obtained by using Lomb's method from the detrended series. The horizontal lines indicate the significance levels, the upper line is the 99% level and the bottom line is the 95% level. Each spectrum has a significant 1 cycle/year frequency peak. Some of the spectra have a peak at a frequency of 2 cycles/year and this can be attributed to asymmetries in the time series.

Figures 5-8 are examples of nowcasts; they show plots of temperature, salinity and density for March, May, August and December 1999. In May 1999, Figure 5, the temperature nowcast shows considerable structure. There is a small pool of cool water (< 4C) inshore and a general gradient to warmer water, deeper offshore. The salinity contains much less structure than the temperature field. Lower salinity water is inshore, coincident with inshore cooler water. As with gradients of temperature, there is also an increase in values of salinity towards the deeper offshore waters.

The density field is almost horizontally uniform (barotropic) across much of the shelf except in the innermost region between GAK 1 and GAK 2 and the doming at and beyond the shelf break.

In May 1999, Figure 6, the temperature nowcast has a more complex structure than in March with intermingled regions of warmer and cooler water. In contrast, the nowcast salinity field is a somewhat smoother version than it was in the March field. The low salinity pool seaward of GAK 1, down to about 100 m, is somewhat larger than in March. The density field has more structure than in March. The doming seen in the March nowcast has moved inshore and the vertical gradient has increased as shown by the crowding of the isopycnals across the shelf.

By August 1999, Figure 7, surface heating has produced a very strong thermocline in the upper 50 to 60 meters all across the shelf. The deeper water is also almost uniform with a small vertical gradient. The only prominent feature below 50 m is the cool water mass on the outermost portion of the line. The salinity nowcast has a small vertical gradient over most of the shelf except for a lens of fresh water in the upper 30 to 50 m in the neighborhood of GAK 1 and GAK 2. The density nowcast field is very similar to the salinity with a small modification in the upper 50 m due to the strong thermocline.

By December 1999, Figure 8, the temperature nowcast has a complex structure similar to that of March 1999. A small lens of warm water exists in the neighborhood of GAK 1. The salinity nowcast is very structured, vertically and horizontally, over the inner half of the shelf and with a lens of low salinity water extending through much of the water column in the region of GAK 1 and GAK 2. The salinity field is almost uniform horizontally over the outer half of the shelf. Finally, the density nowcast is very similar in all of its details to the salinity with some modification due to temperature.

CONCLUSIONS

Overall the NMA technique has produced nowcasts of the temperature, salinity and density, which are spatially smoothed representations of the observations. Because the grid spacing used here is 9 km none of the eigenfunctions have a horizontal structure finer than 18 km. However, the large scale features in the horizontal and much finer scale structures in the vertical are retained in these nowcasts. Also an annual cycle in these fields is reproduced. For temperature, salinity and density the first 13 modes contain around 80% of the variance.

REFERENCES

Eremeev, V. N., L. M. Ivanov, A. D. Kirwan, Jr. and T. M. Margolina, Amount of 137Cs, and its 134Cs radionuclides in the Black Sea produced by the Chernobyl disaster, *J. Environ. Radioact.*, 27, 49-63, 1995.

Lipphardt, B. L., Jr., A. D. Kirwan, Jr., C. E. Grosch, J. K. Lewis and J. D. Paduan, Blending HF radar and model velocities in Monterey bay through normal mode analysis, *J. Geophys. Res.*, 105, 3425-3450, 2000.

ACKNOWLEDGEMENTS

Financial support was provided by NOAA (Grant number NA17RJ1224) through a sub-contract from the University of Alaska (Sub-contract 02-0030).

I would also like to thank Bruce Lipphardt for his help on adapting NMA for a high aspect ratio domain.